Rapid Communications

Unexpected magnetic phase in the weakly ordered spin-$\frac{1}{2}$ chain cuprate Sr_2CuO_3

E. G. Sergeicheva,[1,2] S. S. Sosin,[1,3,*] D. I. Gorbunov,[4] S. Zherlitsyn,[4] G. D. Gu,[5] and I. A. Zaliznyak[5,†]

[1]*P. L. Kapitza Institute for Physical Problems, 117334 Moscow, Russia*

[2]*Low Temperature Laboratory, Department of Applied Physics, Aalto University, P.O. Box 15100, FI-00076 Aalto, Finland*

[3]*National Research University Higher School of Economics, 101000 Moscow, Russia*

[4]*Hochfeld-Magnetlabor Dresden (HLD-EMFL), Helmholtz-Zentrum Dresden-Rossendorf, 01328 Dresden, Germany*

[5]*CMPMSD, Brookhaven National Laboratory, Upton, New York 11973, USA*

(Received 17 November 2019; accepted 23 April 2020; published 15 May 2020)

The magnetic phase diagram of a spin-$\frac{1}{2}$ chain antiferromagnet Sr_2CuO_3 is studied by an ultrasound phase-sensitive detection technique. The system is in the extreme proximity of the Luttinger-liquid quantum-critical point and we observe an unusually strong effect of magnetic field, which is very weak compared to the in-chain interaction, on the Néel ordering temperature. Inside the ordered phase, we detect an unexpected, field-induced continuous phase transition. The transition is accompanied by softening of magnetic excitation observed by electron-spin resonance, which in previous work [E. G. Sergeicheva *et al.*, Phys. Rev. B **95**, 020411(R) (2017)] was associated with a longitudinal (amplitude) mode of the order parameter. These results suggest a transition from a transverse collinear antiferromagnet to an amplitude-modulated spin-density-wave phase in a very weak magnetic field, which is unexpected for a system of weakly coupled Heisenberg spin-$\frac{1}{2}$ chains.

DOI: 10.1103/PhysRevB.101.201107

The ground state of an ideal antiferromagnetic Heisenberg spin-$\frac{1}{2}$ chain is disordered and critical, with a gapless spectrum and power-law decay of spin-spin correlations [1]. A nonzero interchain interaction in material realizations of such chains leads to the formation of long-range antiferromagnetic order at a finite temperature [2]. When the interchain coupling is small, this order can be extremely weak and strongly susceptible to external perturbations, such as magnetic field. Since the properties of an ideal spin-$\frac{1}{2}$ chain are known from the exact solution [1], the mean-field treatment of the exchange coupling between chains [3] allows one to obtain accurate quantitative expressions both for the ground-state order parameter (the staggered magnetization m_0) and the temperature of the magnetic ordering (the Néel temperature T_N) at zero magnetic field,

$$m_0 \approx g\mu_B \times 1.02\sqrt{\frac{J_\perp}{J}}, \quad J_\perp = \frac{T_N}{A\sqrt{\ln(\Lambda J/T_N)}}. \qquad (1)$$

Here, J and $J_\perp$ are intra- and interchain exchange coupling constants, respectively, g is a Landé spectroscopic g-factor, μ_B is a Bohr magneton, and $A \approx 1.28$ and $\Lambda \approx 5.8$ are nonuniversal numerical coefficients.

One of the best realizations of a weakly ordered antiferromagnetic spin-$\frac{1}{2}$ chain system known to date is Sr_2CuO_3. This material has a body-centered orthorhombic crystal structure (space group *Immm*) composed of Cu-O chains running along the b axis of the crystal. The strong Cu-O hybridization along this direction results in an extremely large in-chain superexchange interaction, $J \approx 2800$ K [4–6]. The interchain exchange coupling is significantly reduced due to very small orbital overlaps between Cu-O ensembles in the directions perpendicular to the b axis, thus resulting in an almost ideal spin-chain system. It was found that Sr_2CuO_3 undergoes an ordering transition into a collinear antiferromagnetic state with ordered moments aligned with the b axis at $T_N = 5.5(1)$ K ($T_N \ll J$) [7–9]. The exchange interaction between two nested collinear spin sublattices on a body-centered lattice is fully frustrated, so that on the mean-field level these two subsystems are exchange decoupled. The effective interchain exchange coupling can be evaluated from Eq. (1) as $J_\perp \approx 1.5$ K, yielding a very small ratio $J_\perp/J \lesssim 5 \times 10^{-4}$. The ordered moment estimated from this ratio, $m_0 \approx 0.05\mu_B$, is in good agreement with the experimentally observed value, $\langle\mu\rangle = 0.06\mu_B$, so the system is in very close proximity to the one-dimensional (1D) Luttinger-liquid quantum-critical state.

An electron-spin resonance (ESR) study [7] uncovered two different types of magnetic excitations in the ordered state of Sr_2CuO_3. In addition to conventional pseudo-Goldstone magnons with small gaps induced by weak biaxial anisotropy, a novel spin resonance mode was observed below T_N, which was assigned to a specific gapped longitudinal (amplitude) mode. A longitudinal mode is predicted by chain-mean-field (CMF) theory [3] in proximity to a quantum-critical point and was observed by inelastic neutron scattering in a quasi-one-dimensional (1D) spin-$\frac{1}{2}$ model system $KCuF_3$ [10,11]. The frequency of the new ESR mode decreases with magnetic field, indicating softening at a critical field, $\mu_0 H_c \approx 9.5$ T, above which it increases again. While this observation is compatible with a second-order phase transition, its presence could not be firmly established because of an incomplete gap closure.

*sosin@kapitza.ras.ru
†zaliznyak@bnl.gov

In this Rapid Communication, we study the magnetic phase diagram of Sr_2CuO_3 using a high-sensitivity ultrasonic technique supplemented by additional ESR measurements. We observe an increase of the Néel temperature with magnetic field (by ≈30% at 15 T) consistent with the suppression of quantum fluctuations in a weakly ordered quasi-1D antiferromagnet near quantum criticality [12–16]. In addition, we detect clear anomalies, both in sound velocity and in the attenuation coefficient, which reveal a field-induced phase transition in the field range where the additional gapped ESR mode was found to soften. These anomalies only occur inside an ordered phase and fully disappear above T_N, suggesting the scenario of a continuous phase transition from the transverse Néel order to the longitudinal, amplitude-modulated spin-density wave in magnetic field.

Our experiments were carried out on a high-quality single crystal of Sr_2CuO_3 ($m \simeq 0.1$ g) from the same batch as in Ref. [7]. The sample was cut in a cubic shape with the edges parallel to the three principal axes of the crystal lattice determined by x-ray measurements. ESR measurements were performed on the same sample, which established the equivalence of magnetic spectra to our earlier results [7]. Ultrasonic measurements were carried out at the Dresden High Magnetic Field Laboratory, Helmholtz-Zentrum Dresden-Rossendorf, Germany. The experimental setup was operating as a frequency variable bridge. The relative change in the sound velocity $\Delta v/v$ was assumed to be equal to the relative change in the frequency corresponding to the bridge balance $\Delta f/f = \Delta v/v$, neglecting the change in sample length. Ultrasound waves were generated and registered by $LiNbO_3$ single-crystal resonant piezoelectric transducers with the fundamental frequency ≃27 MHz. All the results described below were obtained for the transverse ultrasound mode propagating along the b axis of the crystal, $k \parallel b$, $u \parallel c$, where k is the wave vector and u is the polarization of the sound.

The temperature dependences of the relative change of the sound velocity $\Delta v/v$ and sound attenuation $\Delta\alpha$ in Sr_2CuO_3 for different magnetic fields applied along the c axis are presented in Figs. 1(a) and 1(b). The temperature dependence indicates spin-lattice coupling, because purely lattice properties are expected to be temperature independent in this range. The sound velocity shows a slight increase with decreasing temperature, by ∼0.01% below 15 K and down to a maximum at 5–6 K, depending on the field, after which it decreases. An exception is the behavior at $\mu_0 H = 9.5$ T with an uprise at low T, which results from the proximity to the field-induced transition discussed below. A maximum is followed by a clear anomaly in the form of a small narrow dip in the middle of the slope, which indicates transition into a magnetically ordered state (indicated by down arrows). The transition is accompanied by a steplike increase of the sound attenuation $\Delta\alpha$ [Fig. 1(b)]. The position of the anomaly, which we associate with T_N, varies from about 4.7 to 6 K, depending on the applied magnetic field.

The magnetic field dependences of $\Delta v/v$ and $\Delta\alpha$ at several constant temperatures from 1.7 to 6 K obtained by sweeping the magnetic field up to 15 T are presented in Figs. 1(c) and 1(d). At the lowest temperature, $T = 1.7$ K, the sound velocity demonstrates a relatively broad humplike feature near

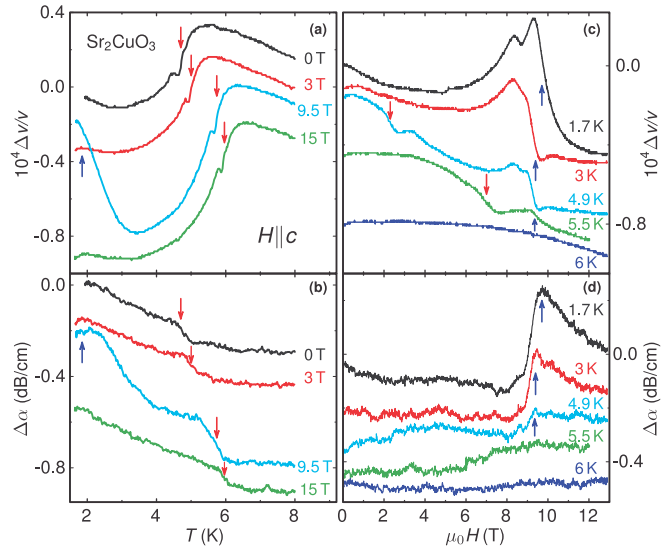

FIG. 1. The temperature dependence of the relative change of sound velocity and sound attenuation of Sr_2CuO_3 measured at several values of external magnetic field [(a), (b)], and their isothermal magnetic field dependence measured at various temperatures [(c), (d)]. Curves, from top to bottom, are vertically shifted for clarity. The magnetic field is applied along the c axis, and magnetic ordering and field-induced transitions are marked by down (↓) and up (↑) arrows, respectively.

$\mu_0 H \approx 9.5$ T, while the sound attenuation shows a (narrower) jumplike anomaly. The position of both features is nearly temperature independent, while they gradually decrease in amplitude with increasing temperature and completely disappear above T_N. The temperature-dependent amplitudes of these features are also reflected in the broad T humps on $\Delta v/v$ and $\Delta\alpha$ curves obtained at 9.5 T and shown by up arrows in Figs. 1(a) and 1(b). On the other hand, the anomaly corresponding to the ordering transition at $T_N(H)$ can also be detected in the isothermal field dependences of $\Delta v/v$ measured at 4.9 and 5.5 K [down arrows in Fig. 1(c)].

Measurements with the same sound propagation geometry were also performed for the magnetic field applied along the b axis. The records of the sound velocity and attenuation versus temperature appeared very similar to the previously discussed data for $H \parallel c$, with similar anomalies corresponding to antiferromagnetic transition temperature $T_N(H)$ [Figs. 2(a) and 2(b)]. However, a remarkable difference is observed in the field sweeps presented in Figs. 2(c) and 2(d). First, both the sound velocity and attenuation exhibit a narrow peak at $\mu_0 H_{sf} \approx 0.5$ T, which corresponds to the spin-flop transition detected in earlier ESR measurements [7]. This peak is followed by a broader, step- or humplike feature around 4 T, which resembles the feature observed in Fig. 1 at $H \parallel c$ near 9.5 T. Similarly to the $H \parallel c$ case, both anomalies do not shift significantly with temperature, but decrease in amplitude and fully disappear above T_N.

Positions of the anomalies observed in all temperature and magnetic field scans are collected in Fig. 3, representing the magnetic phase diagram of Sr_2CuO_3 for two principal directions of the applied field. The points in Fig. 3 correspond to the maximum of the absolute value of the temperature (or

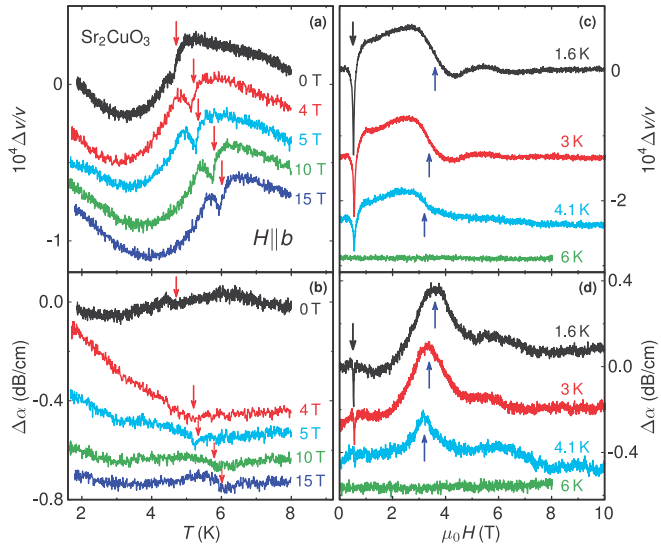

FIG. 2. The relative change of sound velocity and sound attenuation measured vs temperature at several values of external magnetic field [(a), (b)], and vs magnetic field at various temperatures [(c), (d)]. Curves, from top to bottom, are vertically shifted for clarity. The magnetic field is applied along the b axis, and magnetic ordering and field-induced transitions are marked by down (↓) and up (↑) arrows, respectively.

field) derivative $d(\Delta v/v)/dT$ [or $d(\Delta v/v)/dH$] around each anomaly. Another way of determining the phase transition is by the onset of the anomaly in $\Delta\alpha(T, H)$ curves, which gives the results within ± 0.2 K and ± 0.3 T at maximum for temperature and field scans, respectively. This systematic uncertainty is included in the error bars in Fig. 3.

The first notable feature of the phase diagram is the significant increase of the temperature of magnetic ordering under applied field, $\Delta T_N(H) = T_N(H) - T_N(H = 0)$,

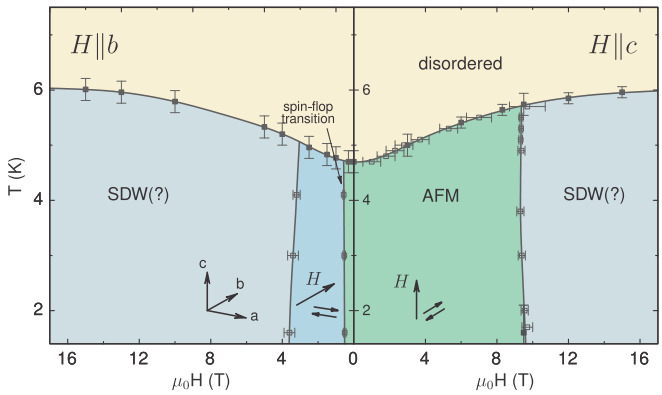

FIG. 3. The magnetic phase diagram of Sr_2CuO_3 obtained from ultrasound measurements at $H \parallel b$ (left panel) and $H \parallel c$ (right panel). Open and solid symbols represent features observed in field and temperature scans, respectively, and error bars represent both the widths and systematic uncertainties in determining the positions of the corresponding features. Lines are shown as a guide for the eye; different magnetic phases are distinguished by colors. Arrows indicate the magnetic field and magnetic moment directions in the a, b, c crystallographic coordinate system shown in the left panel.

which amounts to $\Delta T_N \approx 1.3 \pm 0.1$ K, or approximately $0.3\,T_N(H = 0)$ at a maximum field of 15 T for both field directions. We note that the error in determining the relative shift, ΔT_N, comes from the width of anomalies only and is smaller than the systematic uncertainty of the absolute value of T_N represented by the error bars in Fig. 3. Our data match well the results of specific heat measurements [17] performed in a narrower field range. Being in qualitative agreement with previous results for other quasi-one-dimensional Heisenberg antiferromagnets (see, e.g., Refs. [12–16] and references therein), this finding looks exceptional from a quantitative point of view. For example, a similar relative increase of T_N in an organic spin-$\frac{1}{2}$ quasi-1D system $CuCl_2 \cdot 2NC_5H_5$ ($J/k_B = 13.4$ K, $J_\perp/J \sim 3 \times 10^{-4}$, $T_N = 1.14$ K) [12] is obtained under a magnetic field $\tilde{H} \approx 0.35 H_{\rm sat}$, where $H_{\rm sat} = 4JS/(g\mu_B)$ is a saturation field, while the corresponding field for Sr_2CuO_3 does not exceed $\tilde{H} \approx 2.5 \times 10^{-3} H_{\rm sat}$. A somewhat closer rate of T_N variation under a field ($\tilde{H} \approx 0.02 H_{\rm sat}$) was found in a nearly ideal $S = 5/2$ chain system tetramethylamine manganese trichloride (TMMC), with an even smaller ratio $J_\perp/J = 10^{-4}$. However, the effect we observe in Sr_2CuO_3 is still an order of magnitude larger.

The enhanced initial uprise of T_N under a relatively small ($H \ll H_{\rm sat}$) magnetic field is followed by a flattening of $T_N(H)$ curvature above 10 T, perhaps indicating the presence of an additional energy scale governing magnetic order in Sr_2CuO_3. Among the mechanisms contributing to the initial fast growth, in addition to magnetic field suppression of the frustration on a body-centered lattice (neutron diffraction [7,9,18] indicates degenerate collinear structures in Sr_2CuO_3 below T_N), could be the presence of a tiny amount of impurities [7]. According to NMR experiments [19], a magnetic field can induce local areas of staggered magnetization around impurities, which expand with decreasing temperature, thus possibly stimulating magnetic ordering in a system of weakly coupled spin chains. As for the observed slowing down of $T_N(H)$ dependence, it could be related to the transformation of the magnetic ground state revealed by the field-induced transition reported here.

For the magnetic field applied along the c axis of the crystal, the field range of rapid variation of T_N vs H ends with the field-induced phase transition at $\mu_0 H = 9.6 \pm 0.2$ T. The value of the critical field is nearly temperature independent up to the transition into the paramagnetic phase at $T_N(H)$ (Fig. 3, right panel). For $H \parallel b$, the similar features on the field dependences of sound velocity and attenuation indicating the transition are observed at lower fields, between 3 and 4 T (Fig. 3, left panel).

The ESR measurements presented in Fig. 4 (upper panel) show that the transition at $H \parallel c$ coincides with the softening of the unusual spin excitation mode, which was discovered in our previous ESR experiments and interpreted as the coupled mode of Goldstone spin-wave and the longitudinal (amplitude) mode of the order parameter [7] (no similarly softening resonance mode is seen at $H \parallel b$ in that frequency range). The observed nonmonotonic field dependence can be described by the critical behavior of the resonance frequency, $\nu \propto |H - H_c|$, expected for a continuous second-order phase transition (Fig. 4). A small residual gap introduced to best fit the data might, in principle, reflect a small (1°–2°) deviation of the applied magnetic field from the c axis of the sample.

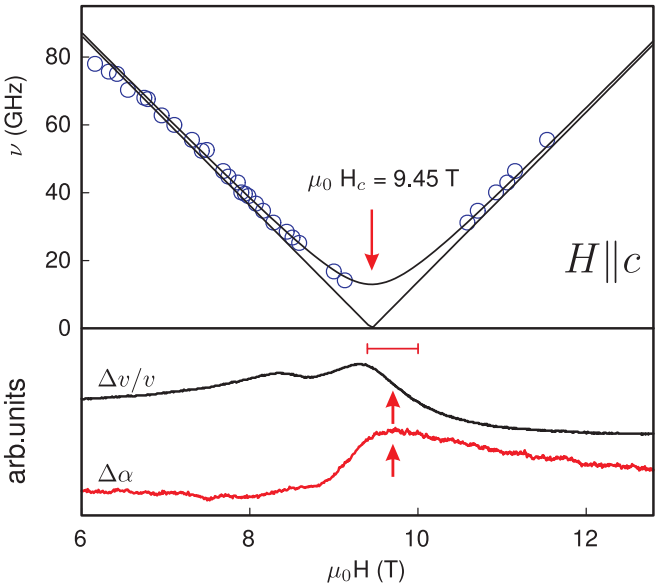

FIG. 4. High-field part of the frequency-field diagram of the magnetic resonance spectrum in the ordered phase of Sr_2CuO_3 measured at $T = 1.5$ K for $H \parallel c$; symbols are experimental points including data from Ref. [7]; the solid line is a fit to the equation $h\nu = \sqrt{(h\delta)^2 + (g_{\rm eff}\mu_B)^2(H - H_c)^2}$ with the critical field $\mu_0 H_c = 9.45$ T (marked by arrow) and the residual gap $\delta = 13$ GHz. The dashed line corresponds to a critical-type linear dependence with $\delta = 0$. The lower panel shows the lowest-temperature curves for $\Delta v/v$ and $\Delta\alpha$ from Figs. 1(c) and 1(d); the anomalies at H_c are pointed out by arrows and their width is shown by a horizontal bar.

Alternatively, this gap could be explained by the mode-repulsive coupling of this excitation with the field-independent pseudo-Goldstone magnon at $\nu \approx 13$ GHz [7], or by Kondo-necklace-type coupling with nuclear spins [20].

Extrapolating the field dependence of the softening mode to $H = 0$, one can estimate its zero-field energy, $h\nu(H = 0) \simeq 0.7 \pm 0.1$ meV. This value compares very favorably with the energy of a longitudinal mode predicted by chain-mean-field theory (CMFT) for weakly coupled spin-$\frac{1}{2}$ chains in proximity to the critical point, $\varepsilon_L = \sqrt{2/3}\,\Delta \approx 0.65$ meV, where $\Delta \approx 6.2 J_\perp \approx 0.8$ meV is a "mass gap" [3]. Inelastic neutron scattering experiments in another $S = \frac{1}{2}$ chain material, $KCuF_3$, provided evidence for the existence of such a mode, albeit heavily damped [10], which hinders its experimental observation by means of magnetic resonance. In Sr_2CuO_3 the softening mode is reasonably sharp, affording its detection by ESR, which is probably due to the remarkable one-dimensionality of this material and its close proximity to the critical point. Attributing this mode to the longitudinal (amplitude) mode of the order parameter, one can tentatively identify the field-induced phase transition accompanied by its softening as a symmetry breaking transition to an amplitude-modulated, longitudinal spin-density-wave (LSDW) state. At $H \parallel b$, the analogous transition is observed in even smaller fields.

An LSDW phase in magnetic field was previously observed in a system of weakly coupled spin-$\frac{1}{2}$ Ising-like XXZ chains [21], which is in agreement with theoretical expectations [22]. For the isotropic Heisenberg model, however, the transverse spin correlation is expected to be dominant and a field-induced transition, which we observe here in low fields, $g\mu_B H_c \ll k_B J$, is markedly unexpected. Our results might signal a breakdown of the simple CMFT by some field-induced mechanism, which might also be "extrinsic" [19,20,23] to the properties of a Luttinger-liquid state of an *ideal, infinite* spin-$\frac{1}{2}$ chain.

In conclusion, ultrasound measurements on Sr_2CuO_3 single crystal were used to obtain the (H, T) magnetic phase diagram in a wide range of temperatures and magnetic fields applied along two principal axes. The results reveal clear anomalies in the sound velocity and attenuation, which identify the temperature of the magnetic ordering transition T_N, the spin flop, and the field-induced magnetic transition inside the ordered phase. The value of the zero-field Néel temperature, $T_N(H = 0) \approx 5$ K, was found to increase markedly with magnetic field, by about 30% at maximum field. The enhanced suppression of quantum fluctuations by a relatively weak magnetic field, $g\mu_B H \ll 4JS$, likely stems from the proximity of the system to the quantum-critical point. Our central result is the field-induced second-order magnetic transition at $g\mu_B H_c \ll J$. The critical field of this transition depends on magnetic field orientation but was found to be nearly temperature independent, with the magnitude of the corresponding anomalies vanishing above T_N. The ESR measurements show that this transition is accompanied by a linear softening and reopening of an unusual gapped mode of magnetic excitation, which can be associated with the longitudinal (amplitude) mode of the order parameter. This suggests a field-induced transformation of the initial collinear antiferromagnet into an amplitude-modulated LSDW state at $g\mu_B H_c \ll J$, which is surprising [22] in the case of the weakly coupled nearly isotropic Heisenberg chains in Sr_2CuO_3 studied here.

The authors are grateful to A. I. Smirnov, L. E. Svistov, V. N. Glazkov, A. Tsvelik, and M. Takigawa for valuable discussions. ESR experiments performed at P. Kapitza Institute were funded by the Russian Science Foundation Grant No. 17-12-01505. S.S.S is grateful to the Basic Research Program of HSE for financial support. We acknowledge support of the HLD at HZDR, member of the European Magnetic Field Laboratory (EMFL), the DFG through SFB 1143, and the excellence cluster *ct.qmat* (EXC 2147, Project ID 39085490). The work at Brookhaven National Laboratory was supported by Office of Basic Energy Sciences (BES), Division of Materials Sciences and Engineering, U.S. Department of Energy (DOE), under Contract No. DE-SC0012704.

[1] A. M. Tsvelik, *Quantum Field Theory in Condensed Matter Physics*, 2nd ed. (Cambridge University Press, Cambridge, UK, 2003).
[2] I. A. Zaliznyak, Nat. Mater. **4**, 273 (2005).
[3] H. J. Schulz, Phys. Rev. Lett. **77**, 2790 (1996).
[4] N. Motoyama, H. Eisaki, and S. Uchida, Phys. Rev. Lett. **76**, 3212 (1996).
[5] H. Suzuura, H. Yasuhara, A. Furusaki, N. Nagaosa, and Y. Tokura, Phys. Rev. Lett. **76**, 2579 (1996).

[6] A. C. Walters, T. G. Perring, J.-S. Caux, A. T. Savici, G. D. Gu, C.-C. Lee, W. Ku, and I. A. Zaliznyak, Nat. Phys. **5**, 867 (2009).
[7] E. G. Sergeicheva, S. S. Sosin, L. A. Prozorova, G. D. Gu, and I. A. Zaliznyak, Phys. Rev. B **95**, 020411(R) (2017).
[8] A. Keren, L. P. Le, G. M. Luke, B. J. Sternlieb, W. D. Wu, Y. J. Uemura, S. Tajima, and S. Uchida, Phys. Rev. B **48**, 12926 (1993).
[9] K. M. Kojima, Y. Fudamoto, M. Larkin, G. M. Luke, J. Merrin, B. Nachumi, Y. J. Uemura, N. Motoyama, H. Eisaki, S. Uchida, K. Yamada, Y. Endoh, S. Hosoya, B. J. Sternlieb, and G. Shirane, Phys. Rev. Lett. **78**, 1787 (1997).
[10] B. Lake, D. A. Tennant, C. D. Frost, and S. E. Nagler, Nat. Mater. **4**, 329 (2005).
[11] B. Lake, D. A. Tennant, and S. E. Nagler, Phys. Rev. B **71**, 134412 (2005).
[12] Y. Endoh, G. Shirane, R. J. Birgeneau, P. M. Richards, and S. L. Holt, Phys. Rev. Lett. **32**, 170 (1974).
[13] W. J. M. de Jonge, J. P. A. M. Hijmans, F. Boersma, J. C. Schouten, and K. Kopinga, Phys. Rev. B **17**, 2922 (1978).
[14] I. U. Heilmann, J. K. Kjems, Y. Endoh, G. F. Reiter, G. Shirane, and R. J. Birgeneau, Phys. Rev. B **24**, 3939 (1981).
[15] I. Zaliznyak, Solid State Commun. **84**, 573 (1992).
[16] M. E. Zhitomirsky and I. A. Zaliznyak, Phys. Rev. B **53**, 3428 (1996).
[17] K. Karmakar, R. Bag, M. Skoulatos, C. Rüegg, and S. Singh, Phys. Rev. B **95**, 235154 (2017).
[18] T. Ami, M. K. Crawford, R. L. Harlow, Z. R. Wang, D. C. Johnston, Q. Huang, and R. W. Erwin, Phys. Rev. B **51**, 5994 (1995).
[19] M. Takigawa, N. Motoyama, H. Eisaki, and S. Uchida, Phys. Rev. B **55**, 14129 (1997).
[20] A. M. Tsvelik and I. A. Zaliznyak, Phys. Rev. B **94**, 075152 (2016).
[21] B. Grenier, V. Simonet, B. Canals, P. Lejay, M. Klanjšek, M. Horvatić, and C. Berthier, Phys. Rev. B **92**, 134416 (2015).
[22] K. Okunishi and T. Suzuki, Phys. Rev. B **76**, 224411 (2007).
[23] S. Eggert, I. Affleck, and M. D. P. Horton, Phys. Rev. Lett. **89**, 047202 (2002).